Proceedings of the International Conference on Heat Transfer and Fluid Flow
Prague, Czech Republic, August 11-12, 2014
Paper No. 59

Viscous Fingering Instabilities In Sinusoidal Time-dependent Flows

Qingwang Yan, Jalel Azaiez
The University of Calgary, Department of Chemical and Petroleum Engineering
Calgary, Alberta Canada T2N 1N4,
qyuan@ucalgary.ca; azaiez@ucalgary.ca

Abstract **-** Miscible non-reactive flow displacements in homogeneous porous media and involving time-dependent sinusoidal injection velocities are modeled. The displacements are examined through full non-linear simulations using the highly accurate Hartley based pseudo-spectral methods. It is found that for the same net injection flow rate, time-dependent sinusoidal flows can actually be more or less unstable than their constant injection velocity counterpart. The effects of three parameters that characterize the sinusoidal profile, namely the amplitude (Γ), the frequency (ω) and the phase (ϕ) were analyzed. It was found that all these parameters affect the flow and result in important changes in the flow structures as well as the breakthrough time, when compared with the constant injection displacement velocity. It was however also found that only the amplitude seems to result in changes in the number of fingers while both the frequency and phase do not affect the number of fingers. These changes in the flow dynamics can be used to control the degree of mixing between the two fluids and to optimize a variety of flow displacements in porous media.

Keywords**:** Flow in porous media, Viscous fingering**,** Time-dependent injection, Numerical simulations.

1. Introduction

Flow instabilities are often observed in processes of displacements of fluids in porous media. Such instabilities develop in the form of complex finger-shaped intrusions at the interface between the two fluids that propagate in both upstream and downstream directions of the flow (Saffman and Taylor, 1958). The instability can be triggered by either viscosity mismatch and is referred to as viscous fingering or density mismatch, where it is known as the Rayleigh-Taylor instability. These fingering phenomena occur in enhanced oil recovery, fixed bed regeneration, groundwater flows, CO_2 sequestration, and soil remediation and filtration, etc. (Hejazi and Azaiez, 2010, 2013). In most cases, viscous fingering is undesirable since it reduces the sweep efficiency, while in others it can be desirable as it promotes mixing. A considerable amount of literature has been published on viscous fingering since it was first examined by Hill (1952). Extensive literature reviews on this instability have been discussed by Homsy (1987) and McCloud and Maher (1995).

To date, most of the existing studies dealing with this type of instability have been limited to flows where the injection velocity is constant. However, in a number of practical applications the displacement velocity is time dependent and hence can result in different flow developments. Examples of such applications are found in trickle-bed reactors (Yaqing et al. 2012) where different time-dependent liquid feed strategies have been adopted to increase the mass transfer rate of the limiting reactant as well as to prevent flow mal-distribution and hot spot formation (Boelhouwer, 2002). Other important applications include a number of enhanced oil recovery (EOR) processes such as the cyclic steam stimulation (CSS) that involves three stages of injection, soaking and production (Mago et al., 2005) as well as the CO_2 huff-and-puff technique that involves cyclic injection of liquid CO_2 for heavy as well as light oil enhanced recovery (Monger et al., 1991). The efficiency of these processes which can be run as either miscible or immiscible depends on the importance and duration of each stage of the cycle.

A very successful application of time-dependent flow rates EOR was investigated by Davidson et al. (1999) and Spanos et al. (2003) who conducted laboratory experiments with a Consistent Pulsing Source (CPS) to generate pulsing water injection to immiscibly displace the oil in sand pack. It was found that time-dependent flow rates can indeed suppress the fingering instability and improve the sweep efficiency in comparison with constant flow rates. Time-dependent flow displacements were also considered in the field of solute transport in groundwater systems. In particular (Singh et al., 2009) examined the effects of seasonal groundwater velocity and water level on contaminant concentration in water and proposed analytical solutions of the one-dimensional concentration transport equation for sinusoidal and exponential velocities. However these authors did not account for the coupled full momentum and mass transport equations and hence the flow instability was not addressed. Recently, Dias et al., (2010a; 2010b; 2012) investigated the possibility of attenuating the fingering instability for immiscible flows in a radial geometry using time-dependent flow rates. They reported the optimal flow rates for linear flow regime and nonlinear flow regime. More recently Yuan and Azaiez (2014) examined the effects of step-size dependent flows on the efficiency and stability of reactive displacements in porous media. The authors showed that it is possible to control the amount of chemical product through a judicious choice of the nature and cycle of the time-dependent displacement.

The present study deals with miscible non-reactive displacements in rectilinear Hele-Shaw cells under sinusoidal flow velocities. The objective of the study is to determine the effects of the frequency, amplitude and phase of the velocity on the hydrodynamic instability and to characterize these effects both qualitatively through concentration contours and quantitatively through the sweep efficiency. The objective is to propose guidelines for the choice of the frequency, amplitude and phase that allow one to control the flow towards either enhancing or attenuating the instability.

2. Mathematical Model and Numerical Procedure

A two-dimensional displacement in which both fluids are incompressible, non-reactive and fully miscible is considered. The flow takes place in the horizontal direction in a homogeneous medium of constant porosity ϕ and permeability K. A schematic of the two-dimensional porous medium is shown in Fig. 1. The length and width of the medium are L and H respectively. The medium is assumed to be initially filled with fluid1 of viscosity μ_1. A miscible fluid2 of viscosity μ_2 is injected from the left-hand side with a velocity u(t) to displace fluid1. The direction of the flow is along the x-axis and the y-axis is parallel to the initial plane of the interface.

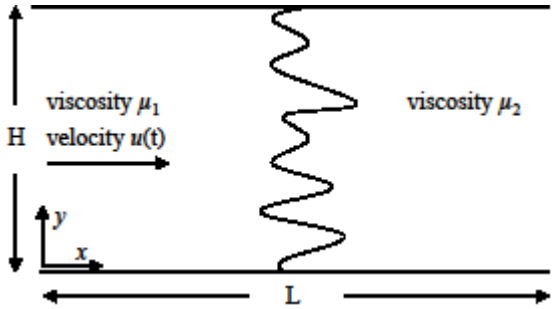

Fig.1. Schematic of the flow.

The model equations are the continuity equation, momentum (Darcy's law) and the transport of the fluids:

$$\nabla.\mathbf{v} = 0 \tag{1}$$

$$\nabla p = -\frac{\mu}{K}\mathbf{v} \tag{2}$$

$$\frac{\partial C}{\partial t} + \frac{\mathbf{v}}{\phi}.\nabla \mathrm{C} = \mathrm{D}\nabla^2 \mathrm{C} \tag{3}$$

In the above equations, **v** is the two-dimensional Darcy velocity; *p* the pressure; *C* the concentration of the displacing fluid; and *D* is the constant diffusion coefficient. The above equations are made dimensionless as in Islam and Azaiez (2005) and Yuan and Azaiez 2014, and are expressed in a Lagrangian reference frame moving with the dimensionless displacement velocity $u_f(t)$. The resulting dimensionless equations (using the same notation) are:

$$\nabla.\mathbf{v} = 0 \tag{4}$$

$$\nabla p = -\mu(\mathbf{v} + \mathrm{u_f}(\mathrm{t})\mathbf{i}) \tag{5}$$

$$\frac{\partial C}{\partial t} + \mathbf{v}.\nabla \mathrm{C} = \nabla^2 \mathrm{C} \tag{6}$$

Two additional dimensionless groups are also involved, namely the Péclet number $Pe = UL/D$ and the cell aspect-ratio $A = L/H$ that appear in the boundary conditions [Hejazi and Azaiez 2013,]. Following previous studies, an exponential concentration dependent viscosity model is adopted to complete the model [Tan and Homsy 1988, Sajjadi and Azaiez (2013)],

$$\mu = exp(RC), \quad R = ln\left(\frac{\mu_2}{\mu_1}\right) \tag{12}$$

where *R* is the log-mobility ratios between the two species. Note that the flow will be unstable for R>0 under an injection process (positive velocity) and stable otherwise. The equations are expressed using a stream-function vorticity formulation, where the velocity field, the stream-function ψ and the vorticity *w* [Hejazi and Azaiez 2013, Yuan and Azaiez 2014]. With this formulation, the continuity equation is satisfied automatically and the governing equations take the forms:

$$\frac{\partial C}{\partial t} + \frac{\partial \psi}{\partial y}\frac{\partial C}{\partial x} - \frac{\partial \psi}{\partial x}\frac{\partial C}{\partial y} = \frac{\partial^2 C}{\partial x^2} + \frac{\partial^2 C}{\partial y^2} \tag{13}$$

$$w = R[\frac{\partial \psi}{\partial x}\frac{\partial C}{\partial x} + \frac{\partial \psi}{\partial y}\frac{\partial C}{\partial y} + \mathrm{u_f}(\mathrm{t})\frac{\partial C}{\partial y}] \tag{14}$$

$$\nabla^2 \psi = -w \tag{15}$$

The partial differential and algebraic equations are solved using a highly accurate pseudo-spectral method based on the Hartley transform [Canuto et al. 1987, Bracewell 2000, Hejazi and Azaiez 2013, Yuan and Azaiez 2014]. This method allows to recast the partial differential equation in time and space into an ordinary differential equation in time. The solution for the time stepping of the diffusive-convective equation was obtained by using a semi-implicit predictor-corrector method along with an operator-splitting algorithm [Islam and Azaiez 2005].

The code was validated by comparing the concentration contours for constant velocity under the same parameters with the studies by Tan and Homsy (1988) and Islam and Azaiez (2005). Furthermore, the convergence of the numerical solution was examined by considering cases with different spatial resolutions varying from 128x128 to 512x512 while varying the time step accordingly. Since a resolution of 256x256 resulted in finger structures similar to those obtained with larger number of grid points, it was adopted in all subsequent simulations. The results will be presented as time sequences of iso-fields of the concentration as well quantitative properties. Note that the time sequences are not always presented at the same time intervals, and only the frames that help in analyzing the effects of the velocity are shown.

In what follows the flow dynamics will be analyzed in the case of are solved numerically in the case of a sinusoidal model where the displacing velocity is set as:

$$u_f(t) = 1 + \Gamma.\sin(2\pi\omega t + \phi) \quad (16)$$

In the above equation Γ is the amplitude, ϕ the phase while ω is the frequency. It should be stressed that the average velocity over a period is one ($\overline{u_f(t)} = 1$), and the discussion will compare the flow developments with a constant injection velocity also equal to one. This implies that the net injected flow in both the time-dependent and constant velocity displacements is the same. Also note that for Γ<1 the velocity is strictly positive at all times while for Γ>1 it can be negative.

3. Results

In this section results are presented for the sinusoidal injection velocity profiles. Unless mentioned otherwise, the following parameters are fixed as: R=3, A=2 and Pe=500. For brevity and illustration purposes, the time sequences will not be always presented necessarily at the same time intervals, and only the frames that reveal new and interesting finger structures that help in the discussion, are shown. In all contours, the red and blue colour fields correspond to the displacing and displaced fluid, respectively. In what follows a comparison between the constant injection and time-dependent velocity flows is presented followed by an analysis of the effects of the magnitude (Γ), the frequency (ω) and the phase (ϕ) of the time-dependent velocity. The results will consist of an analysis of the finger structures as well as of the breakthrough time where the displacing (red) fluid reaches the right-hand side boundary of the domain.

3. 1. Comparison with Constant Injection Flows

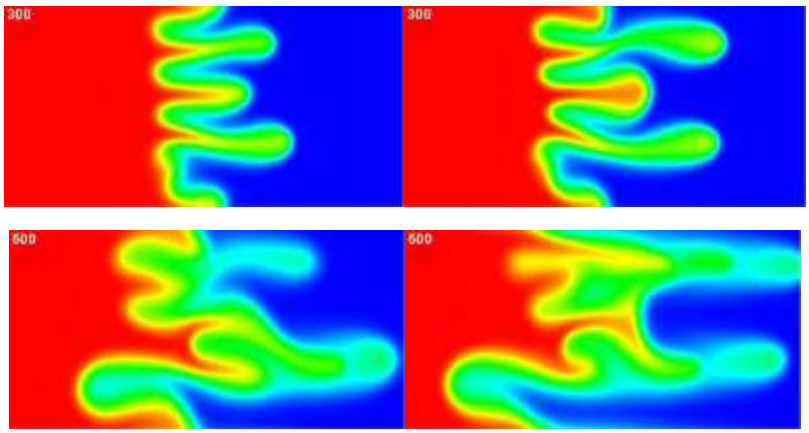

(a) (c)

Fig. 2. Concentration profiles at t=300 and t=500 for (a) constant injection model and (b) cyclic injection model (Γ = 0.5, ω =0.005, ϕ=0).

Figure 2 depicts contours of the concentration for the case of a constant injection velocity (Γ=0) and a sinusoidal velocity (Γ=0.5, ω=0.005, ϕ=0). The period of the sinusoidal model is in this case T=200 and the maximum and minimum velocities are 1.5 and 0.5, respectively. It is obvious that the cyclic injection model is more unstable than that of the constant injection model and that the instability develops earlier in the former case. As a consequence, the displacing fluid is able to breakthrough earlier in the time-dependent displacement case. It should be however noted that the number of fingers has not been affected by the switch to the sinusoidal flow and that the main mechanisms for flow development and interactions are very similar in both flow scenarios. In what follows the effects of the amplitude (Γ) and the frequency (ω) will be analyzed.

3. 2. Effects of the Amplitude (Γ)

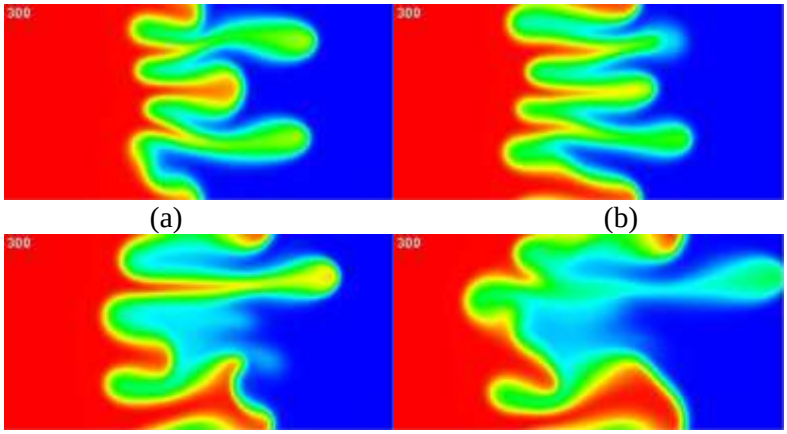

Fig. 3. Concentration profiles of cyclic model with ω =0.005, ϕ=0 at t = 300: (a) Γ=0.5, (b) Γ=1.0, (c) Γ=1.5, (d) Γ=2.0.

In this section the effects of the amplitude are analyzed. As noted earlier, if Γ is larger than one, the displacement may switch to an extraction (negative velocity) regime. During such reversal regime it is expected that the flow instability will be attenuated. Concentration contours are depicted at a time t=300 for four values of Γ. It is clear that the magnitude of the sinusoidal component of the velocity has a strong effects on the instability and the flow development. In particular the number of fingers changes with Γ, and so do the overall finger structures. In particular there is a clear tendency for the fingers to become more complex and to exhibit stronger interactions as the amplitude is increased. This in turn results in shorter breakthrough time for larger amplitudes. It is finally worth noting that even in the cases where the flow reverses to extraction ($u_f(t)<0$), the front between the two fluids is still sharp with strong concentration gradients.

3. 2. Effects of the Frequency (ω)

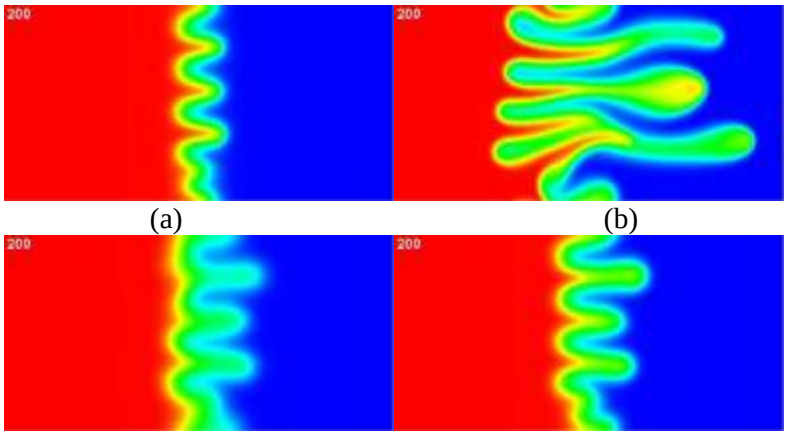

Fig. 4. Concentration profiles of cyclic model with Γ=1.0, ϕ=0 at t=200: (a) ω=0., (b) ω=0.002, (c) ω=0.005, (d) ω=0.01

The effects of the frequency are illustrated in Fig.4 at t=200 and for Γ=1 and ϕ=0. Here too one sees that the flow dynamics are affected by the frequency even though the effects do not seem to be

monotonic. As ω is increased from 2.10^{-3} to 5.10^{-3}, the instability is attenuated and the fingers become more diffuse. Further increase to reverses 10^{-2} the effects and leads to sharp well developed fingers. Still the front is most unstable in the case of the smallest frequency examined. It should be mentioned that the frequency did not affect the number of fingers that develop in the flow.

3. 3. Effects of the Phase (ϕ)

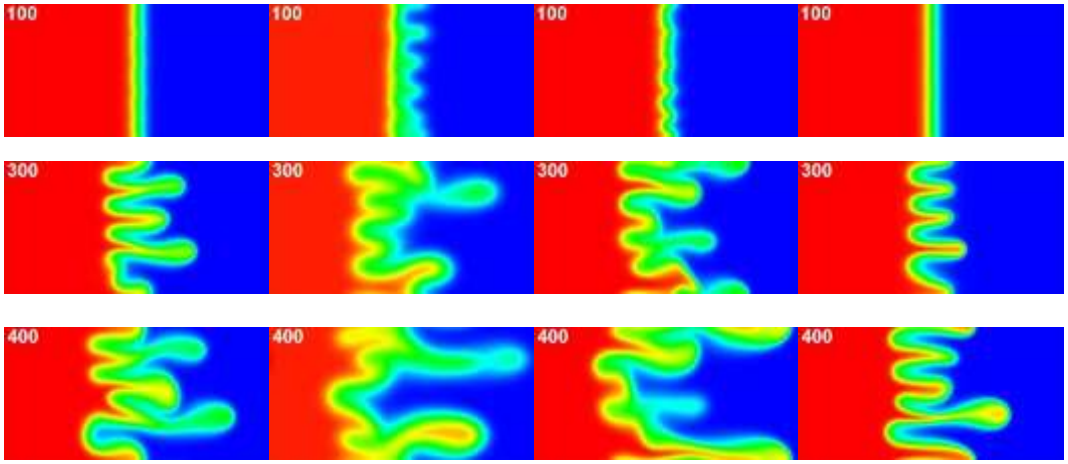

(a) (b) (c) (d)

Fig. 5. Concentration profiles of cyclic model with Γ=2.0, ω=0.01 at t=100, 300 and 400: (a) Constant velocity, (b) ϕ=0, (c) ϕ=π/2, (d) ϕ=π.

The role of the phase ϕ in the flow is shown in Fig. 5 in the case of a sinusoidal velocity with Γ=2 and $\omega=10^{-2}$ corresponding to a period T=100. Results of the constant velocity are also shown for comparison. Note that for Γ=2, the flow will go through stages of injection and extraction and the variation of the phase will control in which of these stages the flow is initiated. Clearly the phase affects the flow and can lead to different finger structures as well as breakthrough times. However similar to what was observed in the case of the frequency, the phase has no effects on the number of fingers. Interestingly, displacement with ϕ=π and hence starting with an extraction followed by an injection result in flow structures that are similar to those of the constant injection velocity. The other two intermediate values of the phase lead to more unstable flows and faster breakthrough times.

4. Conclusion

The effects of a time-dependent sinusoidal displacement velocity on the development of the fingering instability in homogeneous porous media were examined. The dynamics of the flow were analyzed and compared with those arising from a constant injection velocity that results in the same average flow rate. It is found that the time-dependent velocity affects the hydrodynamic instability and in particular can lead to important changes in the number of fingers, the flow structures as well as the flow breakthrough time. The effects of three parameters, namely the velocity amplitude, frequency and phase were analyzed. All three parameters were found to have profound effects on the flow and the breakthrough time. However it was found that only changes in the amplitude can result in changes of the number of fingers while the frequency and phase do not affect the number of fingers. These results can be used to optimize and control the viscous fingering instability through judicious choices of the flow parameters while ensuring that the same amount of fluid is injected in the porous medium.

Acknowledgements

Financial support from the China Scholarship Council (CSC) and the Natural Sciences and Engineering Research Council of Canada (NSERC) are gratefully acknowledged. The authors would like also to acknowledge WestGrid for providing computational resources.

References

Bracewell R. (2000). "The Fourier Transform and its Applications" McGraw-Hill.

Boelhouwer J. G., Piepers H. W., Drinkenburg A. A. H. (2002) Liquid-induced pulsing flow in trickle-bed reactors. Chem. Eng. Sci. 57, 3387-3399.

Canuto C., Hussaini M., Quarteroni A., Zang T. (1987). "Spectral Methods in Fluid Dynamic" Springer.

Davidson B. C., Spanos T., Dusseault M. B., Wang J. (1999) Laboratory experiments on pressure pulse flow enhancement in porous media. "Proc. of the Eighth Petroleum Conf. South Saskatchewan" Regina, Canada, Oct. 18-121, pp 99-90-1–99-9-8

Dias E. O., Parisio F., Miranda J. A. (2010a) Suppression of viscous fluid fingering: A piecewise-constant injection process. Phys. Rev. E 82, 067301-1–067301-4.

Dias E. O., Miranda J. A. (2010b) Control of radial fingering patterns: A weakly nonlinear approach. Phys. Rev. E 81, 016312-1–016312-7.

Dias E. O., Alvarez-Lacalle E., Carvalho M. S. (2012) Minimization of viscous fluid fingering: a variational scheme for optimal flow rates. Phys. Rev. Lett. 109, 144502-1–144502-5.

Hejazi S. H., A., Azaiez J. (2010a) Nonlinear interactions of dynamic reactive interfaces in porous media. Chem. Eng. Sci. 65, 938–949.

Hejazi H., Azaiez, J. (2013) Nonlinear simulation of transverse flow interactions with chemically driven convective mixing in porous media. Water Res. Res. 49, 8, 4607-4618.

Hill, S. (1952) Channeling in packed columns. Chem. Eng. Sci. 1, 247-253.

Homsy G.M. (1987) Viscous Fingering in Porous Media, Ann. Rev. Fluid Mech. 19, 271-311.

Islam N., Azaiez J. (2005) Fully implicit finite difference-pseudo spectral method for the simulation of high mobility-ratio miscible displacements. Int. J. Num. Meth. Fluid. 47, 161-183.

Mago A., Barrufet M., Nogueira M. (2005) Assessing the impact of oil viscosity mixing rules in cyclic steam stimulation of extra-heavy oils. "Proc.. of the SPE Annual Technical Conference and Exhibition" Dallas, USA, Oct. 9-12 pp. SPE 95643-1-7.

McCloud K.V., Maher J.V. (1995) Experimental Perturbations to Saffman-Taylor Flow, Physics Reports 260, 139-185.

Monger T., Ramos J., Thomas J. (1991) Light oil recovery from cyclic CO2 injection: influence of low pressures impure CO2, and reservoir gas. SPE J. 6, 25-32.

Saffman P.G., Taylor G. (1958) The Penetration of a Fluid Into a Porous Medium or Hele-Shaw Cell Containing a More Viscous Liquid, Proc. R. Soc. Lond. *A* 245, 312-329.

Sajjadi M., J. Azaiez J**.** (2013) Scaling and unified characterization of flow instabilities in layered heterogeneous porous media. *Phys. Rev. E.,* 88**,** 033017-1–033017-12.

Singh M., Singh V., Singh P., Shukla D. (2009) Analytical solution for conservative solute transport in one-dimensional homogeneous porous formations with time-dependent velocity. J. Eng. Mech. 135, 1015-1021.

Spanos T., Davidson B.M., Dusseault M., Shand D., Samaroo, M. (2003) Pressure pulsing at the reservoir scale: a new IOR approach. J. Can. Pet. Tech. 42, 16-28.

Tan C., Homsy G. (1988) Simulation of nonlinear viscous fingering in miscible displacement, Phys. Fluids 31, 1330-1338.

Yaqing Z., Xi G., Yaping Z., Zhenghong L. (2012) CFD modeling of methanol to olefins process in a fixed-bed reactor. Powder Tech. 221, 419-430.

Yuan Q., Azaiez J. (2014) Cyclic time-dependent reactive flow displacements in porous media. Chem. Eng. Sci. 109, 136-146.